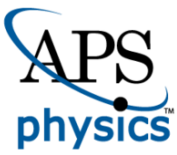

Bounds on the dynamics of periodic quantum walks and emergence of the gapless and gapped Dirac equation

N. Pradeep Kumar, Radhakrishnan Balu, Raymond Laflamme, and C. M. Chandrashekar

Phys. Rev. A **97**, 012116 — Published 17 January 2018

DOI: 10.1103/PhysRevA.97.012116

Bounds on the dynamics of periodic quantum walks and emergence of gapless and gapped Dirac equation

N. Pradeep Kumar,[1] Radhakrishna Balu,[2,3] Raymond Laflamme,[4,5] and C. M. Chandrashekar[1,6,*]

[1] *The Institute of Mathematical Sciences, C. I. T, campus, Taramani, Chennai, 600113, India*
[2] *U.S. Army Research Laboratory, Computational and Information Sciences Directorate, Adelphi, Maryland 20783, USA*
[3] *Computer Science and Electrical Engineering, University of Maryland Baltimore County, 1000 Hilltop Circle, Baltimore, MD 21250, USA*
[4] *Institute for Quantum Computing and Department of Physics and Astronomy, University of Waterloo, Waterloo N2L 3G1, Ontario, Canada*
[5] *Perimeter Institute for Theoretical Physics, Waterloo, N2L 2Y5, ON, Canada*
[6] *Homi Bhabha National Institute, Training School Complex, Anushakti Nagar, Mumbai 400094, India*

We study the dynamics of discrete-time quantum walk using quantum coin operations, $\hat{C}(\theta_1)$ and $\hat{C}(\theta_2)$ in time dependent periodic sequence. For two-period quantum walk with the parameters θ_1 and θ_2 in the coin operations we show that the standard deviation ($\sigma_{\theta_1,\theta_2}(t)$) is same as the minimum of standard deviation obtained from one of the one-period quantum walk with coin operations θ_1 or θ_2, $\sigma_{\theta_1,\theta_2}(t) = \min\{\sigma_{\theta_1}(t), \sigma_{\theta_2}(t)\}$. Our numerical result is analytically corroborated using the dispersion relation obtained from the continuum limit of the dynamics. Using the dispersion relation for one- and two-period quantum walk, we present the bounds on the dynamics of three- and higher period quantum walks. We also show that the bounds for the two-period quantum walk will hold good for the split-step quantum walk which is also defined using two coin operators using θ_1 and θ_2. Unlike the previous known connection of discrete-time quantum walks with the massless Dirac equation where coin parameter $\theta = 0$, here we show the recovery of massless Dirac equation with non-zero θ parameters contributing to the intriguing interference in the dynamics in a totally non-relativistic situation. We also present the effect of periodic sequence on the entanglement between coin and position space.

I. INTRODUCTION

Quantum walk is a generalization of the classical random walk equivalent in a quantum mechanical framework [1–5]. By exploiting the quantum interference in the dynamics, quantum walks outperform the classical random walk by spreading quadratically faster in position space [6, 7]. At certain computational tasks, quantum walks provide exponential speedup [8, 9] over classical computation and are used as a powerful tool in most of the efficient quantum algorithms [10–13]. Both the variants, continuous-time and discrete-time quantum walk have been shown to be universal quantum computation primitive, that is, they can be used to efficiently realize any quantum computation tasks [14, 15]. With the ability to engineer and control the dynamics of discrete-time quantum walk by controlling various parameters in the evolution operators, quantum simulations of localization [16–18], topological bound states [19, 20], relativistic quantum dynamics where the speed of light is mimicked by the parameter of the evolution operator [5, 21–27] and neutrino oscillations [28, 29] has been shown. Quantum walk has also played an important role in modelling the energy transfer in the artificial photosynthetic material [30, 31]. Faster transport [32], graph isomorphism [33] and quantum percolation [34, 35] are few other application where quantum walk has found application.

Experimentally, controlled evolution of quantum walks has also been demonstrated in various physical systems such as NMR [36], trapped ions [37, 38], cold atoms [39] and photonic systems [40–43] making it a most suitable dynamic process which can be engineered for quantum simulations.

Among the two variants of quantum walks, the dynamics of the continuous-time variant are described directly on the position Hilbert space using an Hamiltonian. The dynamics of each step of the discrete-time variant are defined on a Hilbert space composing of both, the position and particle Hilbert space using a combination of unitary quantum coin operation acting only on the particle space followed by a position shift operation acting on both, particle and position space. By exploring different forms of quantum coin and position shift operators in homogeneous [44, 45], periodic [46], quasiperiodic [47, 48] and random [17, 49] sequence, ballistic spreading to the localization of the wavepacket of the particle has been studied. One of the mathematically rigorous approach to understand the asymptotic behaviour of the dynamics is to compute the limit distribution function [50, 51]. In Ref. [46], limit distribution function for two-period quantum walk using two orthogonal matrices as alternate quantum coin operations has been computed. Inspite of the important role of quantum interference in the dynamics of quantum walk it has been shown that the limit distribution of two-period quantum walk is determined by one of the two quantum coin operation (orthogonal matrix).

This is an important observation which needs to be

* chandru@imsc.res.in

explored in more detail to understand the intricacy involved in the dynamics of the periodic quantum walks. Particularly, when two-period quantum walks is shown to produce the dynamics identical to the split-step quantum walk [52] which has been used to simulate topological quantum walks, Dirac-cellular automata [53] and Majorana modes and edge states [52] where both the coin operations play an important role.

Obtaining the limit density function for non-orthogonal unitary matrix as quantum coin operation for two-period and for other $n-$period quantum walk has been a hard task. Even if one succeeds in meticulously obtaining a limit theorem, it will give us an asymptotic behaviour and fails to layout the way evolutions modulate during each sequence of periodic operations.

In this paper we re-visit the dynamics of two-period discrete-time quantum walk using a non-orthogonal unitary quantum coin operations $\hat{C}(\theta_1)$ and $\hat{C}(\theta_2)$. For two-period quantum walk with the parameters θ_1 and θ_2 in the coin operations we show that the standard deviation $(\sigma_{\theta_1,\theta_2})$ is same as the minimum of standard deviation obtained from the one-period quantum walk with coin operations θ_1 or θ_2, $\sigma_{\theta_1,\theta_2} = \min\{\sigma_{\theta_1}, \sigma_{\theta_2}\}$. Our numerical result is analytically corroborated using the dispersion relation obtained from the continuum limit of the dynamics. Though the standard deviations are identical, the spread in position space after t steps is bounded by the $\pm|t\cos(\theta_1)\cos(\theta_2)|$. And the interference pattern is also clearly distinct. This shows up with the prominent presence of both the parameters θ_1 and θ_2 in the differential form of the dynamics expression. We also show that the bounds we obtained for two-period quantum walk will hold good for the split-step quantum walk which is defined using two coin operators using θ_1 and θ_2. Our dispersion relationship approach can be extended to study bounds on the dynamics of three- and higher period quantum walks. Unlike the previous known connection of discrete-time quantum walks with the massless Dirac equation where coin parameter $\theta = 0$, here we show the recovery of gapless (massless) and gapped (massive) Dirac equation with non-zero θ parameters contributing to the intriguing interference in the dynamics in a totally non-relativistic situation. We also study the effect of periodic sequence on the entanglement between coin and position space.

In Sec. II we will give a basic introduction to the operators that define the evolution of discrete-time quantum walk. Using that as a basis we will define the periodic quantum walk and present the numerical results for two-period quantum walk. In Sec. II A, we obtain the dispersion relation for one- and two-period quantum walk and use it arrive at the bounds on the dynamics of two- and three- and higher- period quantum walk. In Sec. III, we present the emerge of Dirac equation from two-period quantum walk and present the enhancement of entanglement for periodic quantum walks in Sec. IV. We conclude with our remarks in Sec. V.

II. PERIODIC QUANTUM WALK

Dynamics of the one dimensional discrete-time quantum walk on a particle with two internal degree of freedom is defined on an Hilbert space $\mathcal{H}_w = \mathcal{H}_c \otimes \mathcal{H}_p$ where the coin Hilbert space $\mathcal{H}_c = span\{|\uparrow\rangle, |\downarrow\rangle\}$ and position Hilbert space $\mathcal{H}_p = span\{|i\rangle\}$, $i \in \mathbb{Z}$ representing the number of position states available to the walker. The generic initial state of the particle, $|\psi\rangle_c$, can be written using a two parameters δ, η in the form,

$$|\psi(\delta,\eta)\rangle_c = \cos(\delta)\,|0\rangle + e^{-i\eta}\sin(\delta)\,|1\rangle\,. \tag{1}$$

Each step of the walk evolution is defined by the action of the unitary quantum coin operation followed by the position shift operator. The single parameter quantum coin operator which is a non-orthogonal unitary and acts only on the particle space can be written in the from,

$$\hat{C}(\theta) = \begin{bmatrix} \cos(\theta) & -i\sin(\theta) \\ -i\sin(\theta) & \cos(\theta) \end{bmatrix}. \tag{2}$$

The position shift operator $\hat{S}$ that translates the particle to the left and/or right conditioned on the internal state of the particle is of the form,

$$\hat{S} = |0\rangle\langle 0| \otimes \sum_{i\in\mathbb{Z}} |i-1\rangle\langle i| + |1\rangle\langle 1| \otimes \sum_{i\in\mathbb{Z}} |i+1\rangle\langle i|\,. \tag{3}$$

The state of the particle in extended position space after t steps of homogeneous (one-period) quantum walk is given by applying the operator $\hat{W} = \hat{S}(\hat{C}\otimes I)$ on the initial state of the particle and the position,

$$|\Psi(t)\rangle = \hat{W}^t\Big[\,|\psi\rangle_c \otimes |x=0\rangle\,\Big] = \sum_x \begin{bmatrix} \psi^{\downarrow}_{x,t} \\ \psi^{\uparrow}_{x,t} \end{bmatrix}. \tag{4}$$

Probability of finding particle at position and time (x,t) will be

$$P(x,t) = \left\|\psi^{\downarrow}_{x,t}\right\|^2 + \left\|\psi^{\uparrow}_{x,t}\right\|^2. \tag{5}$$

Using $P(x,t)$ we can compute the standard deviation (σ) of the probability distribution after t steps of walk.

Two-period quantum walk : To describe the periodic quantum walk we will use two quantum coin operation $C(\theta_1)$ and $C(\theta_2)$. The evolution operator for the t step of two-period quantum walk will be of the form,

$$[\hat{W}_{\theta_2}\hat{W}_{\theta_1}]^{t/2}. \tag{6}$$

For n-period quantum walk the evolution is described using operation $\hat{W}_{\theta_2}$ for every multiple of n steps and $\hat{W}_{\theta_1}$ for all other steps. We should note that the two-period quantum walk we have defined is a time-dependent periodic evolution but for the localized initial state and evolution operators we have defined it is equivalent to position-dependent two-period quantum walk. This equivalence

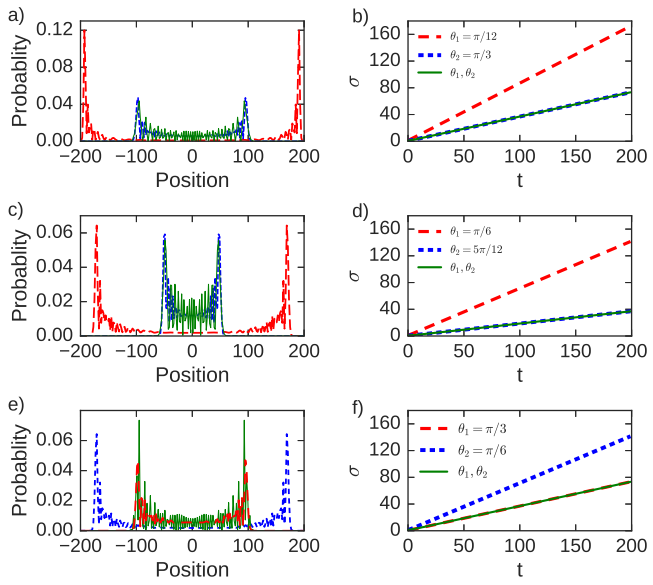

FIG. 1. (Color online) Probability distribution after 200 step of quantum walk using different combination of quantum coin operations and a corresponding standard deviation as a function of time. In (a, c, e) we have plotted the probability distribution in position space for both one- and two-period quantum walk. We can notice that the spread of the probability for two-period case after t steps is bounded by $\pm\min\{t|\cos(\theta_1)|, t|\cos(\theta_2)|\}$. The standard deviation plot in (b, d) shows that $\sigma_{\theta_1,\theta_2}(t) = \sigma_{\theta_2}(t)$ and in (f) $\sigma_{\theta_1,\theta_2}(t) = \sigma_{\theta_1}(t)$. However, the interference pattern is clearly distinct with prominent oscillations for two-period case.

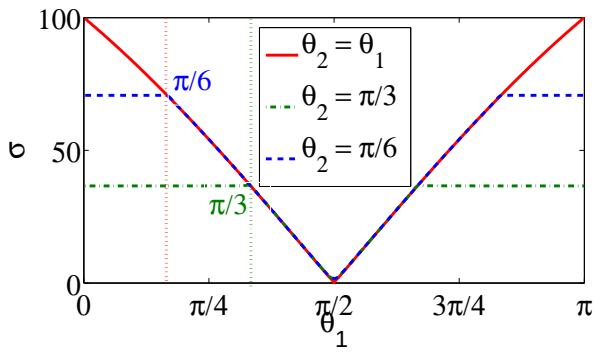

FIG. 2. (Color online) Standard deviation (σ) as function of θ_1 when θ_2 is fixed. With increase in θ_1 we can notice that $\sigma_{\theta_1,\theta_2}(t) = \min\{t|\cos(\theta_1)|, t|\cos(\theta_2)|\}$.

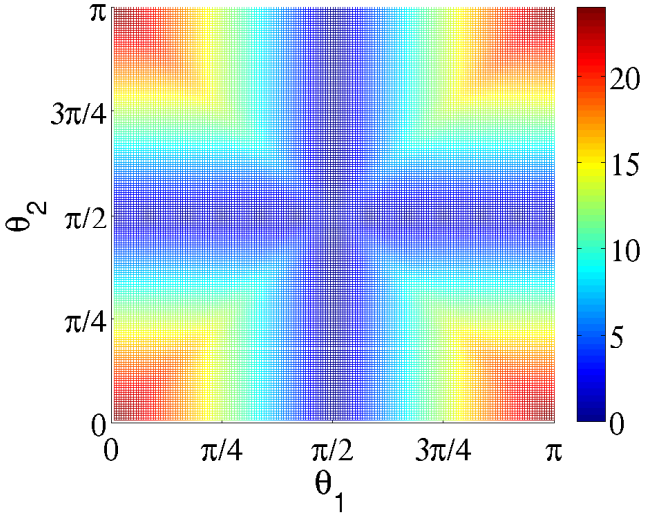

FIG. 3. (Color online) Standard deviation as function of θ_1 and θ_2 after 25 step of quantum walk. With increase in both, θ_1 and θ_2 we can note that $\sigma_{\theta_1,\theta_2}(t) = \min\{t|\cos(\theta_1)|, t|\cos(\theta_2)|\}$.

should be attributed to the probability distribution which will be zero at odd (even) position when t is even (odd). But this equivalence will not hold good to any $n-$ period quantum walk in general.

From earlier results we know that the spread of the one-period quantum walk probability distribution using evolution operation $\hat{W}_\theta$ is bounded between $-t\cos(\theta)$ and $+t\cos(\theta)$ ($\pm t\cos(\theta)$) and $\sigma \propto t|\cos(\theta)|$ [44, 45]. For a two-period walk it looks natural to expect the spread to be bounded somewhere between positions $\pm t\cos(\theta_1)$ and $\pm t\cos(\theta_2)$. But in reality the spread is bounded between $\pm\min\{t|\cos(\theta_1)|, t|\cos(\theta_2)|\}$.

In Fig. 1, the probability distribution and standard deviation (σ) after 200 steps of quantum walk using different values of θ_1 and θ_2, separately (one-period) and together in two-period sequence is presented. We can see that the spread of the probability distribution of the two-period quantum walk $P_{\theta_1,\theta_2}(t)$ is always bounded within the spread of the probability distribution $\min\{P_{\theta_1}(t), P_{\theta_2}(t)\}$ and $\sigma_{\theta_1,\theta_2}(t) = \min\{\sigma_{\theta_1}(t), \sigma_{\theta_2}(t)\}$. But the interference pattern are not identical. In Fig. 2, $\sigma_{\theta_1,\theta_2}$ after 100 steps as function of θ_1 when θ_2 is fixed is presented. In Fig. 3, $\sigma_{\theta_1,\theta_2}$ as function of θ_1 and θ_2 after 25 steps of quantum walk is shown. Analysing the dependence of σ on the two coin parameters we can note that the $\sigma_{\theta_1,\theta_2}(t) \propto \min\{t|\cos(\theta_1)|, t|\cos(\theta_2)|\}$.

In Ref. [46], for combination of orthogonal matrices in two-period quantum walk, the limit distribution ($L_{1,2}(X)$) was computed for specific combination of parameters and shown to be identical to the limit distribution of quantum walk using single coin operation, $L_{1,2}(X) = \min\{L_1(X), L_2(X)\}$. However, from the probability distribution shown in Fig. 1, the interference pattern within in the bound is different and limit distribution function fails to capture that. To get more insight into dynamics of two-period quantum walk and explore the physical significance we will study the dynamic expression at time t and obtain the dispersion relation for it in continuum limit.

A. Dispersion relation and bounds on spread of wavepacket

One-period quantum walk : The state of the particle after $t+1$ number of steps of a one-period discrete-time quantum walk can be written as,

$$|\Psi(t+1)\rangle = \sum_{x=-(t+1)}^{t+1} (\psi^{\downarrow}_{x,t+1} + \psi^{\uparrow}_{x,t+1}) \tag{7}$$

where the left and right propagating components of the particle is given by,

$$\psi^{\downarrow}_{x,t+1} = \cos(\theta)\psi^{\downarrow}_{x+1,t} - i\sin(\theta)\psi^{\uparrow}_{x+1,t} \tag{8a}$$
$$\psi^{\uparrow}_{x,t+1} = -i\sin(\theta)\psi^{\downarrow}_{x-1,t} + \cos(\theta)\psi^{\uparrow}_{x-1,t}. \tag{8b}$$

This can be written in the matrix form,

$$\begin{bmatrix}\psi^{\downarrow}_{x,t+1}\\ \psi^{\uparrow}_{x,t+1}\end{bmatrix} = \begin{bmatrix}\cos(\theta) & -i\sin(\theta)\\ 0 & 0\end{bmatrix}\begin{bmatrix}\psi^{\downarrow}_{x+1,t}\\ \psi^{\uparrow}_{x+1,t}\end{bmatrix} + \begin{bmatrix}0 & 0\\ -i\sin(\theta) & \cos(\theta)\end{bmatrix}\begin{bmatrix}\psi^{\downarrow}_{x-1,t}\\ \psi^{\uparrow}_{x-1,t}\end{bmatrix}. \tag{9}$$

By adding and subtracting the LHS of the Eq. (9) by $\begin{bmatrix}\psi^{\downarrow}_{x,t}\\ \psi^{\uparrow}_{x,t}\end{bmatrix}$ and RHS by $\begin{bmatrix}\cos(\theta) & -i\sin(\theta)\\ -i\sin(\theta) & \cos(\theta)\end{bmatrix}$ we get a difference operator which can be converted to differential operator which will result in the differential equation of the form,

$$\frac{\partial}{\partial t}\begin{bmatrix}\psi^{\downarrow}_{x,t}\\ \psi^{\uparrow}_{x,t}\end{bmatrix} = \begin{bmatrix}\cos(\theta) & -i\sin(\theta)\\ i\sin(\theta) & -\cos(\theta)\end{bmatrix}\begin{bmatrix}\frac{\partial\psi^{\downarrow}_{x,t}}{\partial x}\\ \frac{\partial\psi^{\uparrow}_{x,t}}{\partial x}\end{bmatrix} + \begin{bmatrix}\cos(\theta)-1 & -i\sin(\theta)\\ -i\sin(\theta) & \cos(\theta)-1\end{bmatrix}\begin{bmatrix}\psi^{\downarrow}_{x,t}\\ \psi^{\uparrow}_{x,t}\end{bmatrix}. \tag{10}$$

By reorganising the preceding expression we get a simultaneous equation of the form,

$$\left\{\frac{\partial}{\partial t} - \cos(\theta)\frac{\partial}{\partial x} - (\cos(\theta)-1)\right\}\psi^{\downarrow}_{x,t} + i\sin(\theta)\left\{\frac{\partial}{\partial x}+1\right\}\psi^{\uparrow}_{x,t} = 0 \tag{11a}$$
$$\left\{\frac{\partial}{\partial t} + \cos(\theta)\frac{\partial}{\partial x} - (\cos(\theta)-1)\right\}\psi^{\uparrow}_{x,t} + i\sin(\theta)\left\{\frac{\partial}{\partial x}-1\right\}\psi^{\downarrow}_{x,t} = 0. \tag{11b}$$

For the above expression governing the dynamics of each step of one-period quantum walk in continuum limit, we can seek a Fourier-mode wave like solution of the form

$$\psi_{x,t} = e^{i(kx-\omega t)}, \tag{12}$$

where ω is the wave frequency and k is the wavenumber. Upon substitution into real part of the Eq. (11) we get,

$$\omega = \mp k\cos(\theta) + i[\cos(\theta)-1] \tag{13}$$

and the group velocity will be

$$v^g_1 = \frac{d\omega}{dk} = \mp\cos(\theta). \tag{14}$$

From this we can say that the wavepacket spreads at a rate of $\cos(\theta)$ during each step of the quantum walk and after t steps the spread will be between $\pm t\cos(\theta)$. Though we have used only one form of the quantum coin operation with complex elements in it, the group velocity will be $\propto \cos(\theta)$ even when a most generic unitary operator is used as a quantum coin operation [17].

Two-period quantum walk : For the two-period quantum walk the evolution is driven by two quantum coin operation $\hat{C}(\theta_1)$ and $\hat{C}(\theta_2)$. First, we will write the state at position x and time $t+1$, $\psi^{\downarrow(\uparrow)}_{x,t+1}$ as component of θ_2 at time t,

$$\psi^{\downarrow}_{x,t+1} = \cos(\theta_2)\psi^{\downarrow}_{x+1,t} - i\sin(\theta_2)\psi^{\uparrow}_{x+1,t} \tag{15a}$$
$$\psi^{\uparrow}_{x,t+1} = -i\sin(\theta_2)\psi^{\downarrow}_{x-1,t} + \cos(\theta_2)\psi^{\uparrow}_{x-1,t}. \tag{15b}$$

In the preceding expression, dependency of the state $\psi^{\downarrow(\uparrow)}_{x,t+1}$ on coin parameter θ_1 can be obtained by writing the state $\psi^{\downarrow(\uparrow)}_{x\pm1,t}$ as component of θ_1 at time $(t-1)$,

$$\psi^{\downarrow}_{x+1,t} = \cos(\theta_1)\psi^{\downarrow}_{x+2,t-1} - i\sin(\theta_1)\psi^{\uparrow}_{x+2,t-1} \tag{16a}$$
$$\psi^{\uparrow}_{x+1,t} = -i\sin(\theta_1)\psi^{\downarrow}_{x,t-1} + \cos(\theta_1)\psi^{\uparrow}_{x,t-1} \tag{16b}$$
$$\psi^{\downarrow}_{x-1,t} = \cos(\theta_1)\psi^{\downarrow}_{x,t-1} - i\sin(\theta_1)\psi^{\uparrow}_{x,t-1} \tag{16c}$$
$$\psi^{\uparrow}_{x-1,t} = -i\sin(\theta_1)\psi^{\downarrow}_{x-2,t-1} + \cos(\theta_1)\psi^{\uparrow}_{x-2,t-1} \tag{16d}$$

Now, substituting Eq. (16) into Eq. (15) we obtain,

$$\psi^{\downarrow}_{x,t+1} = \cos(\theta_2)[\cos(\theta_1)\psi^{\downarrow}_{x+2,t-1} - i\sin(\theta_1)\psi^{\uparrow}_{x+2,t-1}] - i\sin(\theta_2)[-i\sin(\theta_1)\psi^{\downarrow}_{x,t-1} + \cos(\theta_1)\psi^{\uparrow}_{x,t-1}] \tag{17a}$$
$$\psi^{\uparrow}_{x,t+1} = -i\sin(\theta_2)[\cos(\theta_1)\psi^{\downarrow}_{x,t-1} - i\sin(\theta_1)\psi^{\uparrow}_{x,t-1}] + \cos(\theta_2)[-i\sin(\theta_1)\psi^{\downarrow}_{x-2,t-1} + \cos(\theta_1)\psi^{\uparrow}_{x-2,t-1}]. \tag{17b}$$

Without loosing any generic feature in the preceding evolution expression we can replace t with $t+1$. After that we can effectively reduce the two step evolution expression using coins with parameter θ_1 and θ_2 to a combined single step evolution expression by replacing $x\pm2$ in RHS by $x\pm1$ and $t+2$ in LHS by $t+1$. This will result in

$$\psi^{\downarrow}_{x,t+1} = \cos(\theta_2)[\cos(\theta_1)\psi^{\downarrow}_{x+1,t} - i\sin(\theta_1)\psi^{\uparrow}_{x+1,t}] - i\sin(\theta_2)[-i\sin(\theta_1)\psi^{\downarrow}_{x,t} + \cos(\theta_1)\psi^{\uparrow}_{x,t}] \tag{18a}$$
$$\psi^{\uparrow}_{x,t+1} = -i\sin(\theta_2)[\cos(\theta_1)\psi^{\downarrow}_{x,t} - i\sin(\theta_1)\psi^{\uparrow}_{x,t}] + \cos(\theta_2)[-i\sin(\theta_1)\psi^{\downarrow}_{x-1,t} + \cos(\theta_1)\psi^{\uparrow}_{x-1,t}]. \tag{18b}$$

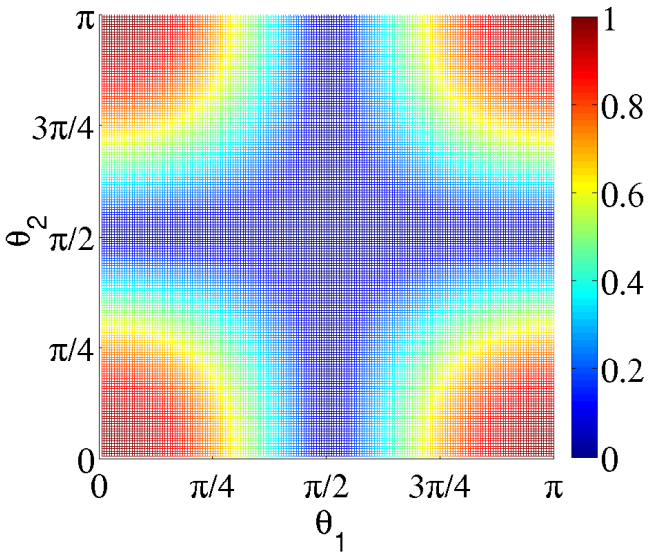

FIG. 4. (Color online) Group velocity obtained from dispersion relation as function of θ_1 and θ_2 for two-period quantum walk. The group velocity obtained in continuum limit of evolution for each step of the walk when multiplied by number of steps of walk it matches with the overall pattern of standard deviation obtained in discrete evolution of the walk.

In matrix form this can be written as,

$$\begin{bmatrix}\psi^{\downarrow}_{x,t+1}\\ \psi^{\uparrow}_{x,t+1}\end{bmatrix} = \begin{bmatrix}-\sin(\theta_2)\sin(\theta_1) & -i\sin(\theta_2)\cos(\theta_1)\\ -i\sin(\theta_2)\cos(\theta_1) & -\sin(\theta_2)\sin(\theta_1)\end{bmatrix}\begin{bmatrix}\psi^{\downarrow}_{x,t}\\ \psi^{\uparrow}_{x,t}\end{bmatrix} + \begin{bmatrix}0 & 0\\ -i\cos(\theta_2)\sin(\theta_1) & \cos(\theta_2)\cos(\theta_1)\end{bmatrix}\begin{bmatrix}\psi^{\downarrow}_{x-1,t}\\ \psi^{\uparrow}_{x-1,t}\end{bmatrix} + \begin{bmatrix}\cos(\theta_2)\cos(\theta_1) & -i\sin(\theta_1)\cos(\theta_2)\\ 0 & 0\end{bmatrix}\begin{bmatrix}\psi^{\downarrow}_{x+1,t}\\ \psi^{\uparrow}_{x+1,t}\end{bmatrix}. \tag{19}$$

By adding and subtracting the LHS of the Eq. (19) by $\begin{bmatrix}\psi^{\downarrow}_{x,t}\\ \psi^{\uparrow}_{x,t}\end{bmatrix}$ and RHS by $\begin{bmatrix}\cos(\theta_2)\cos(\theta_1) & -i\sin(\theta_1)\cos(\theta_2)\\ -i\sin(\theta_1)\cos(\theta_2) & \cos(\theta_2)\cos(\theta_1)\end{bmatrix}$ we get a difference operator which can be converted to differential operator which will result in the differential equation of the form,

$$\frac{\partial}{\partial t}\begin{bmatrix}\psi^{\downarrow}_{x,t}\\ \psi^{\uparrow}_{x,t}\end{bmatrix} = \cos(\theta_2)\begin{bmatrix}\cos(\theta_1) & -i\sin(\theta_1)\\ i\sin(\theta_1) & -\cos(\theta_1)\end{bmatrix}\begin{bmatrix}\frac{\partial\psi^{\downarrow}_{x,t}}{\partial x}\\ \frac{\partial\psi^{\uparrow}_{x,t}}{\partial x}\end{bmatrix} + \begin{bmatrix}\cos(\theta_1+\theta_2)-1 & -i\sin(\theta_1+\theta_2)\\ -i\sin(\theta_1+\theta_2) & \cos(\theta_1+\theta_2)-1\end{bmatrix}\begin{bmatrix}\psi^{\downarrow}_{x,t}\\ \psi^{\uparrow}_{x,t}\end{bmatrix}. \tag{20}$$

The preceding matrix representation can be reorganised

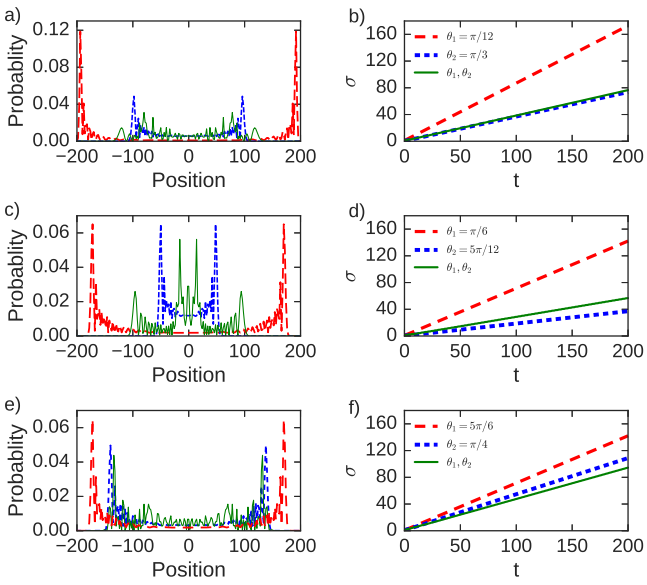

FIG. 5. (Color online) Probability distribution after 200 step of quantum walk for different combination of quantum coin operations and a corresponding standard deviation as a function of time. In (a, c, e) we have plotted the probability distribution in position space for both one- and three-period quantum walk. We can notice that the spread of the probability for three-period case after t steps is always lower than $\pm\max\{t|\cos(\theta_1)|, t|\cos(\theta_2)|\}$ but not bounded by minimum of the two like it was for two-period quantum walk. The standard deviation plot in (b, d, f) shows that $\sigma_{\theta_1,\theta_2}(t)$ will be around $\min\{\sigma_{\theta_1}(t), \sigma_{\theta_2}(t)\}$.

and written as a simultaneous equations,

$$\left\{\frac{\partial}{\partial t} - \cos(\theta_2)\cos(\theta_1)\frac{\partial}{\partial x} - [\cos(\theta_1+\theta_2)-1]\right\}\psi^{\downarrow}_{x,t} + i\left\{\sin(\theta_1)\cos(\theta_2)\frac{\partial}{\partial x} + \sin(\theta_1+\theta_2)\right\}\psi^{\uparrow}_{x,t} = 0 \tag{21a}$$

$$\left\{\frac{\partial}{\partial t} + \cos(\theta_2)\cos(\theta_1)\frac{\partial}{\partial x} - [\cos(\theta_1+\theta_2)-1]\right\}\psi^{\uparrow}_{x,t} - i\left\{\sin(\theta_1)\cos(\theta_2)\frac{\partial}{\partial x} - \sin(\theta_1+\theta_2)\right\}\psi^{\downarrow}_{x,t} = 0. \tag{21b}$$

For the above expression effectively governing the dynamics of the two-period quantum walk in continuum limit, we can seek a Fourier-mode wave like solution of the form $\psi_{x,t} = e^{i(kx-\omega t)}$. Upon substitution into real part of the Eq. (21) we get,

$$\omega = \mp k\cos(\theta_2)\cos(\theta_1) + i[\cos(\theta_1+\theta_2)-1] \tag{22}$$

and the group velocity will be

$$v_2^g = \frac{d\omega}{dk} = \mp\cos(\theta_2)\cos(\theta_1). \tag{23}$$

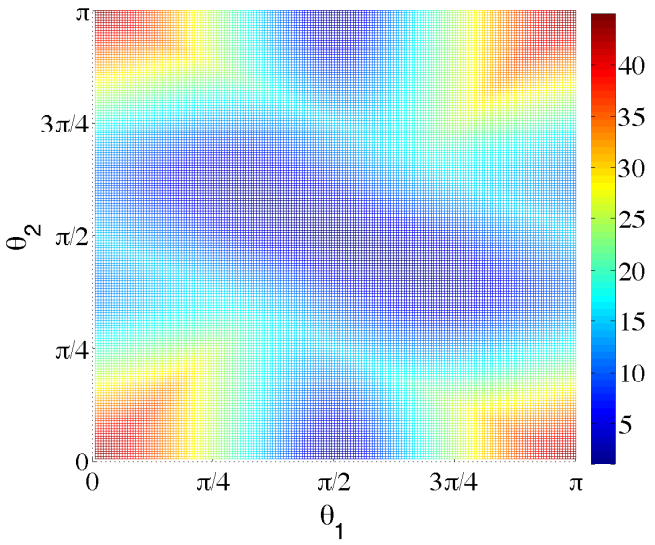

FIG. 6. (Color online) Standard deviation as function of θ_1 and θ_2 after 45 steps of three-period quantum walk. Except for θ's where $|\cos(\theta_1)| \approx |\cos(\theta_2)|$ and close to unity, standard deviation is very low. This can be attributed to multiple peaks in the distribution where peaks with higher probability is closer to origin.

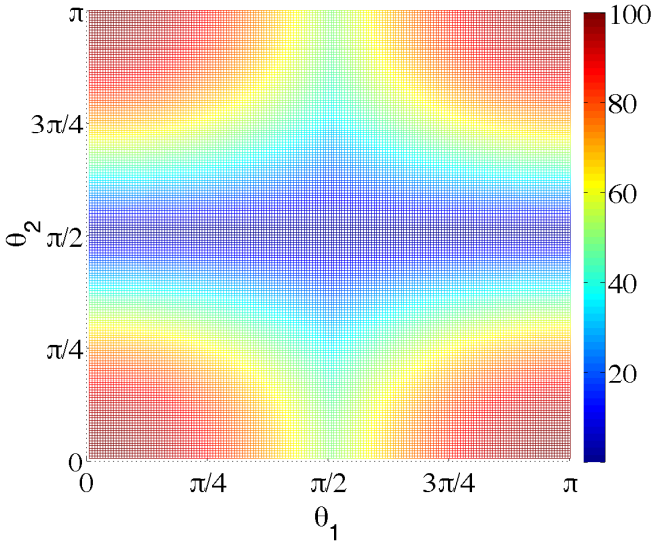

FIG. 7. (Color online) Spread of the probability distribution in position space after 100 step of three-period quantum walk as function of θ_1 and θ_2. This bound on the spread in obtained from the maximum of group velocity v_3^g.

In Fig. 4 we have plotted group velocity for two-period quantum walk, $v_2^g(\theta_1, \theta_2)$. This gives an effective displacement of the wavepacket for each step of two-period quantum walk when two step evolution using θ_1 and θ_2 is combined to one effective step evolution. Comparing Fig. 4 and Fig. 3, v_g and σ as function of θ_1 and θ_2 we can see an identical pattern and only when the dominance of one θ over the other happen, the transition is smooth for v_g. This is due to the continuum approximation we made in the analytics.

From the expression for group velocity, Eq. (23), we can infer that

$$|v_2^g| \leq \min\{|\cos(\theta_1)|, |\cos(\theta_2)|\}. \tag{24}$$

Therefore, the bound on the group velocity sets the bound on the standard deviation, $\sigma(t) \propto t|v_2^g|$. This bound on the group velocity and standard deviation corroborates with the bounds we obtained from the numerical analysis.

Three- and n−period quantum walk : First three step of three-period quantum walk using two quantum coin operation $\hat{C}(\theta_1)$ and $\hat{C}(\theta_2)$ is implemented with the evolution operator in sequence,

$$\hat{W}_{3P} = \hat{W}_{\theta_2}\hat{W}_{\theta_1}\hat{W}_{\theta_1}. \tag{25}$$

In Fig. 5, probability distribution after 200 step of three-period quantum walk is presented and spread of the probability after t steps is always lower than $\pm\max\{t|\cos(\theta_1)|, t|\cos(\theta_2)|\}$ but not bounded by minimum of the two like it was for two-period quantum walk. The standard deviation plot in (b, d, f) shows that $\sigma_{\theta_1,\theta_2}(t)$ will be around $\min\{\sigma_{\theta_1}(t), \sigma_{\theta_2}(t)\}$ and does not match explicitly. In Fig. 6, standard deviation as function of θ_1 and θ_2 after 45 steps of three-period quantum walk is shown. Except for evolution parameter where $|\cos(\theta_1)| \approx |\cos(\theta_2)|$ and close to unity, standard deviation is very low. This can be attributed to multiple peaks in the distribution where peaks with higher probability is closer to origin.

Unlike two-period case where only two peaks were seen in the probability distribution, multiple peaks can emerge in the three- and $n-$period quantum walk (see Fig. 8). This can result in mismatch between the linear scaling of group velocity with the standard deviation. However, group velocity can give us a definite bound on the maximum spread of the probability distribution in position space for three- and $n-$ period quantum walk.

Evolution operator for first three step of three-period walk can be re-written as,

$$\hat{W}_{3P} = \hat{W}_{2P}\hat{W}_{\theta_1}, \tag{26}$$

where $\hat{W}_{2P}$ represent the two-period operator sequence for which we already know the dispersion relation and v_2^g (Eq. (23)) when it is treated as an effective one step evolution. Extrapolating v_1^g and v_2^g from one-period and two-period quantum walk we can write the group velocity for three period walk in the form,

$$v_3^g = \frac{\pm(v_1^g + v_2^g)}{2} = \pm\frac{1}{2}\Big[\cos(\theta_1) \pm \cos(\theta_1)\cos(\theta_2)\Big]. \tag{27}$$

For any given values of θ's, we can get multiple valid value

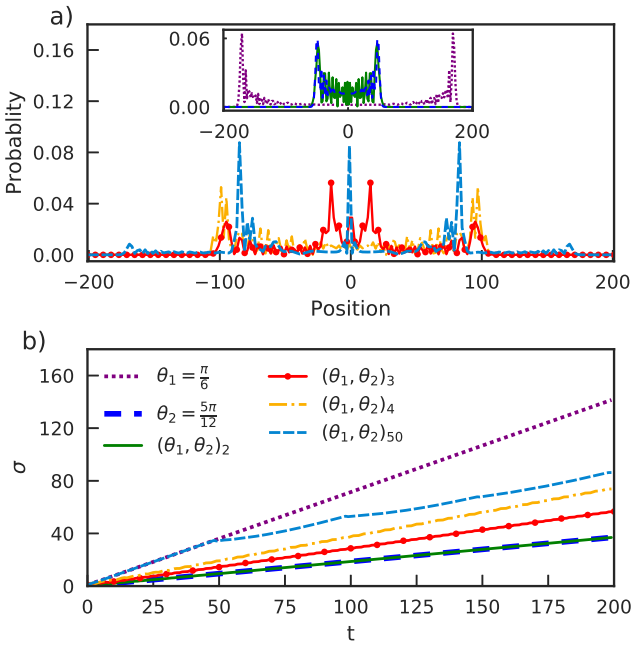

FIG. 8. (Color online) Probability distribution and standard deviation after 200 steps of $n-$period quantum walk. In (a) the probability distribution for three-period, four-period, and fifty-period quantum walk is shown. The inset shows the position probability distribution for two-period and when coin is homogeneous (one-period) with coin parameter θ_1 and θ_2 . The standard deviation (b) shows only two-period evolution is bounded by θ_1 for three-period and four-period it is bounded between θ_2 and θ_1. We can verify that the spread in probability distribution is bounded by maximum of group velocity for all $n-$period quantum walks.

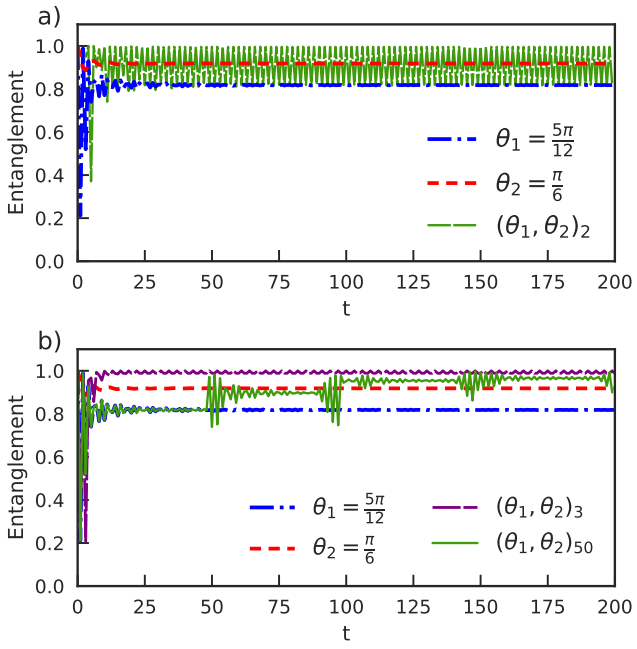

FIG. 9. (Color online) Entanglement between the particle and position for 200 steps for one-, two-, three- and fifty-period quantum walk. For two-period quantum walk (a), in contrast to standard deviation, the mean value of entanglement is bounded around the maximum of the two on-period quantum walk. For three-period quantum walk, entanglement reaches a maximum possible value and from larger $n-$ period quantum walk we can see how the enhancement happens when quantum coin operation with θ_2 is introduced periodically.

for v_3^g . This can be interpreted as wavepacket simultaneously evolving with different v_3^g resulting in multiple peaks in the probability distribution. Among the possible values for v_3^g the contribution for maximum spread in position space will be from,

$$\max|v_3^g| = \frac{1}{2}\Big[|\cos(\theta_1)| + |\cos(\theta_1)\cos(\theta_2)|\Big]. \tag{28}$$

From the preceding expression we can conclude that the bound on the spread of the wavepacket in position space after t step of three-period walk will be,

$$\pm\, t\, \max|v_3^g| = \frac{\pm t}{2}\Big[|\cos(\theta_1)| + |\cos(\theta_1)\cos(\theta_2)|\Big]. \tag{29}$$

In Fig. 7, bounds on the spread of the probability distribution in position space after 100 step of three-period quantum walk as function of θ_1 and θ_2 is shown. This bound on the spread in obtained from the maximum of group velocity v_3^g. By substituting finite values for θ_1 and θ_2 into Eq. (29) we can confirm that the bounds we get from maximum of group velocity matches with the maximum range of spread of probability distribution obtained from numerical evolution (Fig. 5(a, c, e) and Fig. 8).

For $n-$period quantum walk, the spread of the probability distribution will be bounded by,

$$\pm t\, \max|v_n^g| = \frac{\pm t}{(n-1)}\Big[(n-2)|\cos(\theta_1)| + |\cos(\theta_1)\cos(\theta_2)|\Big]. \tag{30}$$

In Fig. 8, probability distribution and standard deviation after 200 steps of $n-$period quantum walks is shown. We can verify that the spread in probability distribution is bounded by maximum of group velocity for all $n-$period quantum walks.

III. TWO-PERIOD QUANTUM WALK, SPLIT-STEP QUANTUM AND DIRAC EQUATION

Split-step quantum walk was first introduced to define topological quantum walk [20] and was show to simulate Dirac cellular automata [53]. Recently, the decomposed

form of split-step quantum walk was shown to be equivalent to two-period quantum walk and simulate Majorana modes and edge states [52]. In this section, staring from the split-step quantum walk we arrive at the differential equation form of the evolution equation which is equivalent to two-period quantum walk evolution equation. From this we can establish that all bounds applicable to two-period quantum walk will hold good for split-step quantum walk and equivalent form of Dirac equations.

Each step of split-step quantum walk is a composition of two half step evolutions,

$$\hat{W_{ss}} = \hat{S}_+(\hat{C}(\theta_2)\otimes I)\hat{S}_-(\hat{C}(\theta_1)\otimes I), \tag{31}$$

where $\hat{C}(\theta_1)$ and $\hat{C}(\theta_2)$ are quantum coin operation and we will define it in same form as Eq. (2). Position shift operator are defined as,

$$\hat{S}_- = |0\rangle\langle 0|\otimes\sum_{i\in\mathbb{Z}}|i-1\rangle\langle i| + |1\rangle\langle 1|\otimes\sum_{i\in\mathbb{Z}}|i\rangle\langle i| \tag{32a}$$

$$\hat{S}_+ = |0\rangle\langle 0|\otimes\sum_{i\in\mathbb{Z}}|i\rangle\langle i| + |1\rangle\langle 1|\otimes\sum_{i\in\mathbb{Z}}|i+1\rangle\langle i|. \tag{32b}$$

The state at any position x and time $t+1$ after the operation of $\hat{W}_{ss}$ at time t will be $\psi_{x,t+1} = \psi^{\downarrow}_{x,t+1} + \psi^{\uparrow}_{x,t+1}$, where

$$\begin{aligned}\psi^{\downarrow}_{x,t+1} &= \cos(\theta_2)[\cos(\theta_1)\psi^{\downarrow}_{x+1,t} - i\sin(\theta_1)\psi^{\uparrow}_{x+1,t}]\\ &\quad -i\sin(\theta_2)[-i\sin(\theta_1)\psi^{\downarrow}_{x,t} + \cos(\theta_1)\psi^{\uparrow}_{x,t}]\end{aligned} \tag{33a}$$

$$\begin{aligned}\psi^{\uparrow}_{x,t+1} &= -i\sin(\theta_2)[\cos(\theta_1)\psi^{\downarrow}_{x,t} - i\sin(\theta_1)\psi^{\uparrow}_{x,t}]\\ &\quad +\cos(\theta_2)[-i\sin(\theta_1)\psi^{\downarrow}_{x-1,t} + \cos(\theta_1)\psi^{\uparrow}_{x-1,t}].\end{aligned} \tag{33b}$$

The preceding expression is identical to Eq. (18) which we have obtained for two-period quantum walk. Therefore, the differential equation form of the evolution will be same as Eq. (20). By controlling the parameters θ_1 and θ_2 we can arrive at the Dirac equations for massless and massive particles.

1. Multiplying Eq. (20) by $i\hbar$ and setting $\theta_1 = 0$ and θ_2 to a small value (mass of sub-atomic particles) we recover Dirac equation in the form,

$$i\hbar\left[\frac{\partial}{\partial t} - \left(1-\frac{\theta_2^2}{2}\right)\begin{bmatrix}1&0\\0&-1\end{bmatrix}\frac{\partial}{\partial x} + i\theta_2\begin{bmatrix}0&1\\1&0\end{bmatrix}\right]\begin{bmatrix}\psi^{\downarrow}_{x,t}\\ \psi^{\uparrow}_{x,t}\end{bmatrix} \approx 0. \tag{34}$$

2. By choosing θ_1 and θ_2 such that $\cos(\theta_1+\theta_2) = 1$ in Eq. (20), and multiplying by $i\hbar$ we get an expression identical to Dirac equation of massless particle,

$$i\hbar\left[\frac{\partial}{\partial t} - \cos(\theta_2)\begin{bmatrix}\cos(\theta_1) & -i\sin(\theta_1)\\ i\sin(\theta_1) & -\cos(\theta_1)\end{bmatrix}\frac{\partial}{\partial x}\right]\begin{bmatrix}\psi^{\downarrow}_{x,t}\\ \psi^{\uparrow}_{x,t}\end{bmatrix} = 0. \tag{35}$$

Here the co-efficient of the position derivative is a more general Hermitian matrix which depicts the oscillation of the spin (eigen state) during the dynamics.

3. By choosing θ_1 to be extremely small and corresponding θ_2 such that $\cos(\theta_1+\theta_2) = 1$ in Eq. (20), and multiplying by $i\hbar$ we get the Dirac equation in the form,

$$i\hbar\left[\frac{\partial}{\partial t} - \cos(\theta_2)\begin{bmatrix}1&0\\0&-1\end{bmatrix}\frac{\partial}{\partial x}\right]\begin{bmatrix}\psi^{\downarrow}_{x,t}\\ \psi^{\uparrow}_{x,t}\end{bmatrix} \approx 0. \tag{36}$$

In Ref. [53], it was shown that $\theta_1 = 0$ and small value of θ_2 is required to recover Dirac cellular automata from split-step quantum walk and both $\theta_1 = \theta_2 = 0$ to recover massless Dirac equation. Here, we have shown the other possible configurations of non-zero θ values where we can recover massless Dirac equation. From bounds on two-period quantum walk (equivalently split-step walk) we can imply that the spread of wavepacket for massive and Massless, that is, gapped and gapless Dirac equation of the form, Eq. (34) and Eq. (36), respectively is bounded by the parameter θ_2. The spread will be very wide for the former and small for the later (remain around the origin). For the massless Dirac equation with general Hermitian matrix, Eq. (35), the spread will be bounded by $\min\{\cos(\theta_1), \cos(\theta_2)\}$.

IV. ENTANGLEMENT IN PERIODIC QUANTUM WALKS

Entanglement of particle with position during quantum walk evolution has been reported in many earlier studies. Entanglement during temporal disordered (spatial disorder) quantum walk is reported to higher (lower) than the homogenous (one-period) quantum walk [17]. In homogenous quantum walk, mean value of entanglement generated is independent of the initial state of the particle. But in the split-step quantum walk, the dependence of mean value of entanglement is prominently visible [53]. Therefore, for two-period quantum walk, entanglement behaviour will be identical to the one reported in Ref. [53]. In this section we will see how the entanglement manifests and reaches maximum value for $n-$period quantum walk.

As we have considered only a pure quantum state evolution in this study, we will use the partial entropy as a measure of entanglement, which is enough to give correct measure of entanglement for the pure state evolution with unitary operators. We will first take partial trace with respect to $\mathcal{H}_p$-space (position space) of time evolved state $= Tr_p(\rho(t)) := \rho_c(t)$. Then according our measure the entanglement at time t is given by,

$$-Tr_c[\rho_c(t)\log_2\{\rho_c(t)\}], \tag{37}$$

the suffix c represents the coin space.

In Fig. 9, we present the entanglement between the particle and position space as a function of time for one- and two- and $n-$period quantum walk. For two-period quantum walk, in contrast to standard deviation, the

mean value of entanglement is bounded around the maximum of the two one-period quantum walk. For three-period quantum walk, entanglement reaches a maximum value, higher than the entanglement due to both, one-period quantum walk is seen. This is also in contrast to the way, spread in position space and standard deviation decreases for periodic quantum walks. For higher period quantum walk we can see that the change of coin induces the increase in entanglement.

V. CONCLUSION

In this work we have presented the dynamics of time dependent periodic quantum walk. In particular, we have shown the way probability distribution spread, standard deviation increase and entanglement vary for periodic quantum walk and show the way they are bounded when compared with the dynamics properties of homogeneous (single coin driven) quantum walk. For two-period quantum walk with the parameters θ_1 and θ_2 in the coin operations we show that $\sigma_{\theta_1,\theta_2} = \min\{\sigma_{\theta_1}, \sigma_{\theta_2}\} \propto \min\{t|\cos(\theta_1)|, t|\cos(\theta_2)|$. Our numerical results was corroborated with analytical analysis from the dispersion relation of the two-period quantum walk. Re-visiting the split-step quantum walk dynamics we have also shown that the all the bounds we have presented for two-period quantum walk will be identical to the split-step quantum walk. Unlike computing limit density function which is meticulously hard, we have used the dispersion relation from one-period and two-period quantum walk to understand the bounds on the spread of the wavepacket for $n-$ period quantum walk, $\frac{\pm t}{(n-1)}\Big[(n-2)|\cos(\theta_1)| + |\cos(\theta_1)\cos(\theta_2)|\Big]$. By re-visiting the connection of quantum walks with Dirac equation, we have shown configuration of periodic quantum walk evolution which can recover Dirac equation for both, massive and massless particles with non-zero coin parameter θ. Thus, the evolution configuration that results in emergence of gapless and gapped Dirac equation. This can contribute to quantum simulation of dynamics in Dirac materials. We also showed that the periodic sequence will enhance the entanglement between the coin and position space in the quantum walk dynamics.

Depending on the convenience of the experimental system, either of the, two-period or split-step quantum walk can be used for quantum simulations of various low-energy and higher energy particle dynamics defined by Dirac equations. The bounds we have presented with further help in understanding the transition from diffusive to localised state.

Acknowledgment:

CMC and NPK would like to thank Department of Science and Technology, Government of India for the Ramanujan Fellowship grant No.:SB/S2/RJN-192/2014. CMC and RL would also acknowledge the support from US Army Research Laboratory.

[1] G. V. Riazanov, Sov. Phys. JETP **6**, 1107âĂŞ1113 (1958).
[2] R. P. Feynman, Quantum mechanical computers, Found. Phys. **16**, 507-531 (1986).
[3] K. R. Parthasarathy, The passage from random walk to diffusion in quantum probability, Journal of Applied Probability **25**, 151-166 (1988).
[4] Y. Aharonov, L. Davidovich, and N. Zagury, Quantum random walks, Phys. Rev. A **48**, 1687-1690 (1993).
[5] D. A. Mayer, From quantum cellular automata to quantum lattice gases, J. Stat. Phys **85**, 551 (1996).
[6] J. Kempe, Quantum random walks: an introductory overview, Contemp. Phys **44.4**, 307-327, (2003).
[7] E. S. Venegas- Andraca, Quantum walks: a comprehensive review, Quantum. Info. Process **11**, 1015 (2012).
[8] A. M. Childs, R. Cleve, E. Deotto, E. Farhi, S. Gutmann and D. A. Spielman, Exponential algorithmic speedup by a quantum walk, STOC '03 Proceedings of the thirty-fifth annual ACM symposium on Theory of computing (pp. 59-68) (2003).
[9] A. M. Childs and J. Goldstone, Spatial search by quantum walk, Phys. Rev. A **70**, 022314 (2004).
[10] A. Ambainis, Quantum walk algorithm for element distinctness, SIAM Journal on Computing **37**, 210-239 (2007).
[11] F. Magniez, M. Santha, and M. Szegedy, Quantum algorithms for the triangle problem, SIAM Journal on Computing **37**, 413-424 (2007).
[12] H. Buhrman and R. Špalek, Quantum verification of matrix products, In Proceedings of the seventeenth annual ACM-SIAM symposium on Discrete algorithm, pp. 880-889. Society for Industrial and Applied Mathematics (2006).
[13] E. Farhi, J. Goldstone and S. Gutmann, A Quantum Algorithm for the Hamiltonian NAND Tree, Theory of Computing, Article 8 pp. 169-190 (2008).
[14] A. M. Childs, Universal computation by quantum walk, Phys. Rev. Lett. **102**, 180501 (2009).
[15] N. B. Lovett, S. Cooper, M. Everitt, M. Trevers and V. Kendon, Universal quantum computation using the discrete-time quantum walk, Phys. Rev. A **81**, 042330 (2010).
[16] A. Joye, Dynamical localization for d-dimensional random quantum walks, Quantum Inf. Process **11**, 1251 (2012).
[17] C. M. Chandrashekar, Disorder induced localization and enhancement of entanglement in one- and two-dimensional quantum walks, arXiv:1212.5984 (2012).

[18] C. M. Chandrashekar and Th. Busch, Localized quantum walks as secured quantum memory, Euro. Phys. Lett **110**, 10005 (2015).

[19] H. Obuse, and N. Kawakami, Topological phases and delocalization of quantum walks in random environments, Phys. Rev. B **84**, 195139 (2011).

[20] T. Kitagawa, M. S. Rudner, E. Berg and E. Demler, Exploring topological phases with quantum walks, Phys. Rev. A **82**, 033429 (2010).

[21] F. W. Strauch, Relativistic quantum walks, Phys. Rev. A **73**, 054302 (2006).

[22] C. M. Chandrashekar, S. Banerjee, and R. Srikanth, Relationship between quantum walks and relativistic quantum mechanics, Phys. Rev. A **81**, 062340 (2010).

[23] C. M. Chandrashekar, Two-component Dirac-like Hamiltonian for generating quantum walk on one-, two- and three-dimensional lattices. Scientific. Reports **3**, 2829, (2013).

[24] G. Di Molfetta, M. Brachet and F. Debbasch, Quantum walks as massless Dirac fermions in curved space-time, Phys. Rev. A **88**, 042301 (2013).

[25] G. Di Molfetta, M. Brachet and F. Debbasch, Quantum walks in artificial electric and gravitational fields, Physica A **397**, 157âĂŞ168 (2014).

[26] P. Arrighi, S. Facchini and M. Forets, Quantum walks in curved spacetime, arXiv:1505.07023 (2015).

[27] A. Pérez, Asymptotic properties of the Dirac quantum cellular automaton, Phys. Rev. A **93**, 012328 (2016).

[28] A. Mallick, S. Mandal, C. M. Chandrashekar, Neutrino oscillations in discrete-time quantum walk framework, Eur. Phys. J. C **77**, 85 (2017).

[29] G. Di Molfetta, A. Pérez, Quantum walks as simulators of neutrino oscillations in a vacuum and matter, New. J. Phys. **18**, 103038 (2016).

[30] G. S. Engel *et al.*, Evidence for wavelike energy transfer through quantum coherence in photosynthetic systems, Nature **446**, 782 (2007).

[31] M. Mohseni, P. Rebentrost, S. Lloyd and A. Aspuru-Guzik, Environment-assisted quantum walks in photosynthetic energy transfer, J. Chem. Phys **129**, 174106 (2008).

[32] S. Hoyer and D. A. Meyer, Faster transport with a directed quantum walk, Phys. Rev. A **79**, 024307 (2009).

[33] B. L. Douglas and J. B. Wang, Classical approach to the graph isomorphism problem using quantum walks, J. Phys. A: Math. Theor **41**, 075303 (2008).

[34] C. M. Chandrashekar and Th. Busch, Quantum percolation and transition point of a directed discrete-time quantum walk, Scientific Reports **4**, 6583 (2014).

[35] B. Kollar, T. Kiss, J. Novotny, I. Jex, Asymptotic dynamics of coined quantum walks on percolation graphs, Phys. Rev. Lett **108**, 230505 (2012).

[36] C. A. Ryan, M. Laforest, J. C. Boileau and R. Laflamme, Experimental implementation of a discrete-time quantum random walk on an NMR quantum-information processor, Phys. Rev. A **72**, 062317 (2005).

[37] H. Schmitz, R. Matjeschk, Ch. Schneider, J. Glueckert, M. Enderlein, T. Huber, T. Schaetz, Quantum walk of a trapped ion in phase space, Phys. Rev. Lett **103**, 090504 (2009).

[38] F. Zahringer, G. Kirchmair, R. Gerritsma, E. Solano, R. Blatt, and C. F. Roos, Realization of a Quantum Walk with One and Two Trapped Ions, Phys. Rev. Lett **104**, 100503 (2010).

[39] K. Karski, L. Foster, J. M. Choi, A. Steffen, W. Alt, D. Meschede, and A. Widera, Quantum walk in position space with single optically trapped atoms, Science **325**, 174 (2009).

[40] A. Schreiber, K. N. Cassemiro, V. Potocek, A. Gabris, P. Mosley, E. Andersson, I. Jex, and Ch. Silberhorn, Photons Walking the Line: A Quantum Walk with Adjustable Coin Operations, Phys. Rev. Lett, **104**, 05502 (2010).

[41] M. A. Broome, A. Fedrizzi, B. P. Lanyon, I. Kassal, A. Aspuru-Guzik, and A. G. White, Discrete Single-Photon Quantum Walks with Tunable Decoherence, Phys. Rev. Lett **104**, 153602 (2010).

[42] A. Peruzzo *et. al*, Quantum Walks of Correlated Photons, Science **329**, 1500 (2010).

[43] H. B. Perets, Y. Lahini, F. Pozzi, M. Sorel, R. Morandotti and Y. Silberberg, Realization of Quantum Walks with Negligible Decoherence in Waveguide Lattices, Phys. Rev. Lett **100**, 170506 (2008).

[44] A. Nayak and A. Vishwanath, Quantum walk on a line, arXiv:0010117 (2000).

[45] C. M. Chandrashekar, R. Srikanth, and R. Laflamme, Optimizing the discrete time quantum walk using a SU(2) coin, Phys. Rev. A **77**, 032326 (2010).

[46] T. Machida and N. Konno, Limit theorem for a time-dependent coined quantum walk on the line, F. Peper et al. (Eds.): IWNC 2009, Proceedings in Information and Communications Technology **2**, 226 (2010).

[47] P. Xue, H. Qin, B. Tang and B. C Sanders, Observation of quasiperiodic dynamics in a one-dimensional quantum walk of single photons in space, New. J. Phys **16**, 053009 (2014).

[48] N. Lo Gullo, C. V. Ambarish, Th. Busch, L. Dell'Anna, C. M. Chandrashekar, Dynamics and energy spectra of aperiodic discrete-time quantum walks, Phys. Rev. E **96**, 012111 (2017).

[49] A. Ahlbrecht, H. Vogts, A. H. Werner, and R. F. Werner, Asymptotic evolution of quantum walks with random coin, J. Math. Phys **52**, 042201 (2011).

[50] N. Konno, T. Luczak, E. Segawa, Limit measures of inhomogeneous discrete-time quantum walks in one dimension, Quantum. Info. Process **12**, 33, (2013).

[51] N. Konno, Localization of an inhomogeneous discrete-time quantum walk on the line, Quantum. Info. Process **9**, 405 (2010).

[52] W. W. Zhang, S. K. Goyal, C. Simon, B. C. Sanders, Decomposition of split-step quantum walks for simulating Majorana modes and edge states, Phys. Rev. A **95**, 052351 (2017).

[53] A. Mallick, C. M. Chandrashekar, Dirac Quantum Cellular Automaton from Split-step Quantum Walk, Scientific Reports **6**, 25779 (2016).